Chapter

Wideband Systems with Energy Harvesting Units for 5G, Medical and Computer Industry

Albert Sabban

Abstract

Demand for green energy is in tremendous growth in the last decade. The continuous growth in production of portable RF systems increase the consumption of batteries and electrical energy. Batteries and conventional electrical energy increase the environmental pollution. Compact wideband efficient antennas are crucial for energy harvesting commercial portable sensors and systems. Small antennas have low efficiency. The efficiency of 5G, IoT communication and energy harvesting systems may be improved by using wideband efficient antennas. Ultra-wideband portable harvesting systems are presented in this chapter. This chapter presents new Ultra-Wideband energy harvesting system and antennas in frequencies ranging from 0.15GHz to 18GHz. Three wideband antennas cover the frequency range from 0.15GHz to 18GHz. A wideband metamaterial antenna with metallic strips covers the frequency range from 0.15GHz to 0.42GHz. The antenna bandwidth is around 75% for VSWR better than 2.3:1. A wideband slot antenna covers the frequency range from 0.4GHz to 6.4GHz. A wideband fractal notch antenna covers the frequency range from 6GHz to 18GHz. Printed passive and active notch and slot antennas are compact, low cost and have low volume. The active antennas may be employed in energy harvesting portable systems. The antennas and the harvesting system components may be assembled on the same, printed board. The antennas bandwidth is from 75–200% for VSWR better than 3:1. The antennas gain is around 3 dBi with efficiency higher than 90%. The antennas electrical parameters were computed by using 3D electromagnetic software in free space and in vicinity of the human body. There is a good agreement between computed and measured results.

Keywords: green energy, energy harvesting, wideband antennas, metamaterial antenna, notch, slot antennas

1. Introduction

This chapter presents new Ultra-Wideband programmable communication systems with energy harvesting modules and efficient compact antennas in frequencies ranging from 0.15GHz to 18GHz. In last twenty years free space energy in the forms of light, heat, vibration, electromagnetic waves, muscle motion and other type of energy, is used to produce green energy. Methods to produce green electricity from these different types of energy sources have been presented and investigated [1–4].

Energy harvesting systems provide green energy and may eliminate the need to replace batteries every day and the usage of power cords. Batteries and cables waste pollute the environment. To use as much free space energy as possible it is important to harvest the electromagnetic power from wideband range of wireless communication systems. In these cases, we should use ultra-wideband antennas. Moreover, a programmable array with two to four antennas can harvest energy from 100 MHz to 18GHz. The energy harvesting antenna must satisfy the requirements related to the system application. Due to considerably low-power electromagnetic energy densities in free space, highly efficient antennas are significant. Patch, slot, and dipole antennas were employed to harvest electromagnetic energy [4–7]. Printed antennas are used in communication and medical system [4–25]. Wideband slot and notch antennas may be used in wideband harvesting energy systems. Slot and notch antennas have low volume, low weight, low cost, and are flexible. Moreover, a compact low-cost energy harvesting network and matching network may be produced by integrating the system RF components with the resonators on the same board. Printed compact antennas are widely presented in the literature in the last twenty years as referred in [7–25]. Human body effect on the electrical performance of wearable medical system and antennas at microwave frequencies should be considered. Electrical properties of human tissues have been presented in several papers such as [26–27]. Several wearable antennas were presented in books and papers in the last years as referred in [27–36]. Printed notch and slot antennas for harvesting energy applications are rarely presented in the literature. New ultra-wideband wearable antennas for 5G, IOT and medical RF systems with energy harvesting units are presented in this chapter.

2. Energy harvesting systems for 5G, IOT, medical and computer industry

In the last decade there is a significant increase in the amount of electromagnetic energy in the air. Almost every person has a cellular phone tablet and other communication devices. In electromagnetic energy harvesting systems, the electromagnetic waves propagating in free space may be received by harvesting antennas and converted to electric energy that is used to charge batteries and for other devices. The expected amount of radio wave in the air in 2019 was 33 Exa-bytes, EB, per month. However, the expected amount of radio wave in the air in 2025 is expected to be 164 Exa-bytes per month, see **Table 1**. **Table 1** presents the expected amount of radio wave in the air for 2G, 3G, 4G, and 5G networks. 5G is forecast to account for 45% of global mobile data traffic by 2025. Computations per KWh from 1985 to

Year	Total amount of radio wave in free space EB per month	Amount of radio wave in free space EB per month 2G, 3G, 4G	Amount of radio wave in free space EB per month 5G
2015	4.4	4.4	0
2017	11	11	0
2019	33	33	0
2021	60	50	10
2023	100	75	25
2025	164	85	79

Table 1.
Expected amount of radio wave in free space from 2015 up to 2025.

2018 are listed in **Table 2**. Energy sources used in harvesting systems are listed in **Table 3**. Communication services such as television, GSM, wireless local area networks, WLAN, and Wi-Fi covers the frequency range from 0.2 GHz to 5.4 GHz. Wireless communication systems operate in the frequencies from 700 MHz to 2700 MHz. Medical systems operate in the frequencies from 200 MHz to 1200 MHz. WLAN systems operate in the frequencies from 5400 MHz to 5900 MHz.

RF energy is inversely proportional to distance and therefore drops as the distance from a source is increased. Harvested power from RF energy sources is lower than 0.1 mW/cm^2. Electromagnetic energy harvesting system is shown in **Figure 1**. A programmable array with 3 to 4 antennas can harvest RF energy from 0.15GHz up to 18GHz. The received RF energy may be combined after transformed to DC power.

The RF energy harvesting system consists of antennas, matching and feed networks, rectifying circuit, and a rechargeable battery. The harvesting energy system operates as a dual mode RF harvesting system. The harvesting unit can be part of a medical, IOT, computer, and smartphone. The LNA DC bias voltages are supplied by the receiving system The Low Noise Amplifier is part of the. The energy coupled to the transmitting built in test, -20 dB, may be harvested and used to charge a battery. We can calculate the energy harvesting link budget by using Eq. (1), [8], if

Year	Computations per KWh (1E+09)
1985	50
1987	100
1992	1000
1997	10,000
2003	100,000
2008	1,000,000
2010	15,000,000
2012	20,000,000
2014	30,000,000
2016	40,000,000
2018	50,000,000

Table 2.
Computations per KWh from 1985 to 2018.

Energy source	Type	Efficiency	Estimated harvested power
Electromagnetic	0.3 – 5GHz Wi-Fi, WLAN	∼50%	1 μW/cm^2 0.01 μW/cm^2
Wireless 1-3GHz	Wireless	∼50%	0.1 up to 5 mW/cm^2
Light	Outdoor or Indoor	10 ∼ 25%	150 mW/cm^2
Thermal	Human Industrial	∼0.1% ∼3%	60 μW/cm^2 ∼1–10 mW/cm^2
Vibration	∼Hz–human ∼kHz–machines	20 ∼ 50%	∼4 μW/cm^3 ∼800 μW/cm^3

Table 3.
Energy sources used in harvesting systems.

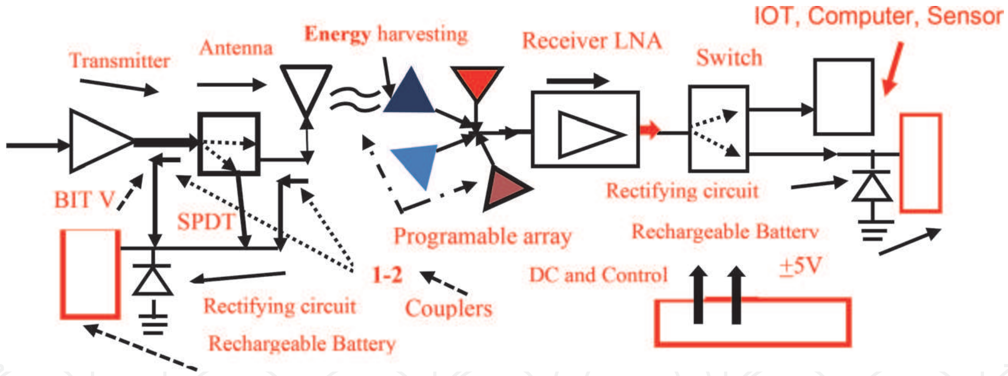

Figure 1.
Dual mode programmable Array energy harvesting system.

the antennas are matched and there are no losses in the medium. However, if the antennas are not matched and the RF energy propagates in a lossy media, we can calculate the energy harvesting link budget by using Eq. (2), [8]. Wireless smart phone using standard 802.11 can transmit up to 1Watt. Free Space Loss (Lp) represents propagation loss in free space. Losses due to attenuation in atmosphere, La = $e^{-\alpha r}$, should be accounted for in the transmission equation.

$$P_r = P_t G_t G_r \left(\frac{\lambda}{4\pi R}\right)^2 \tag{1}$$

$$P_r = P_t G_r G_t \left(\frac{\lambda}{4\pi r}\right)^2 \left(1 - |\Gamma_t|^2\right)\left(1 - |\Gamma_r|^2\right) \left|a_t a_r^*\right|^2 e^{-\alpha r} \tag{2}$$

The attenuation constant is α. Where, $L_p = \left(\frac{4\pi R}{\lambda}\right)^2$. The received power may be given as: $P_r = \frac{P_t G_t G_r}{L_p}$. Losses due to polarization mismatch, Lpol = $|a_t a_r|^2$, should also be accounted. Losses associates with receiving antenna, Lra, and with the receiver, Lr = $(1 - |\Gamma_r|^2)$, should be accounted in computation of transmission budget. Losses associates with the transmitting antenna as written as, Lta = $(1 - |\Gamma_t|^2)$. Where: Γ_r is the reflection coeficient of the receiving antenna.

$$P_r = \frac{P_t G_t G_r}{L_p L_a L_{ta} L_{ra} L_{pol} L_o L_r} \tag{3}$$

Γ_t *is the reflection coeficient of the transmitting antenna*.Pt = Pout/Lt, see Eq. (3), [8].

Pt = Transmitting antenna power. Lt = Loss between power source and antenna.

EIRP = Effective isotropic radiated power. Where, EIRP = Pt Gt, see Eq. (4), [8]. Where,

$$\begin{aligned} P_r &= \frac{P_t G_t G_r}{L_p L_a L_{ta} L_{ra} L_{pol} L_{other} L_r} \\ &= \frac{EIRP \text{ x } G_r}{L_p L_a L_{ta} L_{ra} L_{pol} L_{other} L_r} \\ &= \frac{P_{out} G_t G_r}{L_t L_p L_a L_{ta} L_{ra} L_{pol} L_{other} L_r} \end{aligned} \tag{4}$$

Gain, G, in dB; and L, Loss in dB is written as: $G = 10 \cdot \log\left(\frac{P_{out}}{P_{in}}\right)$ dB $L = 10 \log\left(\frac{P_{in}}{P_{out}}\right)$ dB.

The received power Pr in dBm may be calculated by using Eq. (5), [8]. The received power Pr is referred to as the "Carrier Power". Personal Computer Memory *Cards* using standard 802.11 can transmit up to 100 mW.

$$P_r = EIRP - L_{ta} - L_p - L_a - L_{pol} - L_{ra} - L_{other} + G_r - L_r \qquad (5)$$

Figure 2 presents a wideband receiving system, 500 MHz -18GHz, with energy harvesting units.

Figure 3 presents a wideband transmitting system, 500 MHz to 18GHz, with energy harvesting units.

Three wideband antennas are employed in the receiving and transmitting systems presented in **Figures 2** and **3**. The first antenna covers frequencies from 150 MHz to 0.5GHz. The second antenna covers frequencies from 500 MHz to 6GHz. The third antenna covers frequencies from 6GHz to 18GHz. The receiving and transmitting systems can harvest energy from 150 MHz to 18GHz. Almost in every transmitting or receiving channel part of the energy, -10 dB to -20 dB, is coupled to a built-in test port. This RF energy can be transformed to DC energy and can be used to charge electrical devices. In the receiving channel the received RF energy from 150 MHz to 6GHz is transferred via a wideband combiner or SPDT to a second SPDT that is connected to the 6GHz to 18GHz antenna. The output of the second SPDT is connected to a third wideband SPDT via a wideband LNA. The LNA is part of the receiving channel. The output of the third SPDT transfer the receiving

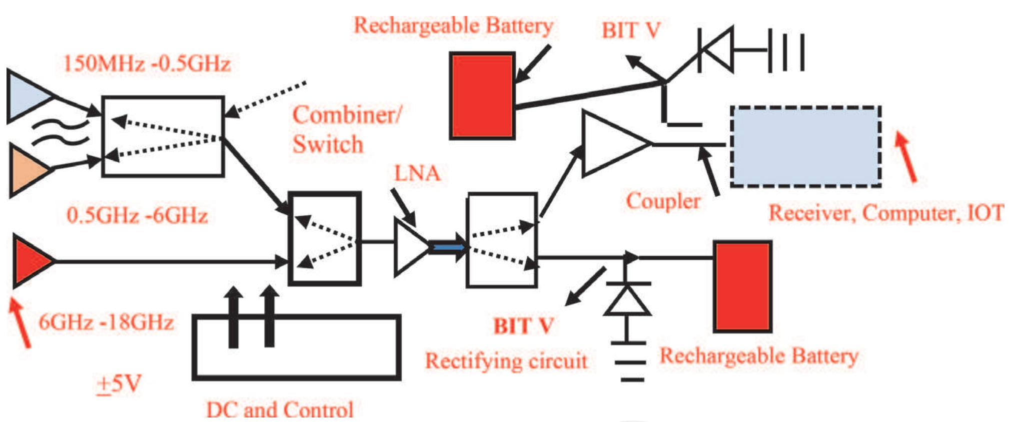

Figure 2.
Wideband harvesting receiving programmable Array system.

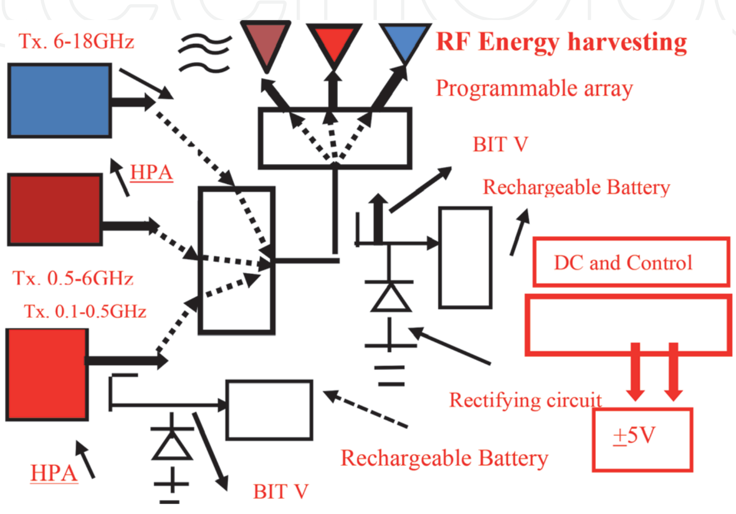

Figure 3.
Optimized harvesting transmitting programmable Array system.

RF energy to the receiving channel or to the harvesting system. A wideband amplifier transfers the received RF signal to the receiver. The received RF energy is coupled, -10 dB to -20 dB, is coupled to a Built in Test port. This RF energy is transformed to DC energy and may be used to charge electrical devices. A wideband switching matrix connects three power amplifiers to three transmitting antennas. The first antenna covers the frequency range from 150 MHz to 0.5GHz. The second antenna covers frequencies from 500 MHz to 6GHz. The third antenna covers frequencies from 6GHz to 18GHz. A DC unit supply the bias voltages to the amplifiers and control the switching matrix state. The harvesting system may consist one to three antennas according to the system requirements. The antennas may cover the frequency range from 150 MHz to 6.4GHz only.

3. Wideband 150 MHz to 0.4GHz, energy harvesting antenna

RF energy in the frequency range from150MHz to 500 MHz may be harvested by a wideband compact metamaterial antenna as presented in **Figure 4**. The antenna is a dual polarized printed dipole and slot antennas with Split Ring Resonators and metallic strips. The microstrip loaded dipole antenna with SRR provides horizontal polarization. The slot antenna provides vertical polarization. The dipole feed network is printed on the first layer. The radiating dipole with SRR is printed on the second layer. The thickness of each layer is 0.8 mm. The length of the antenna with SRR is 19.8 cm. The SRR ring width is 1.4 mm the spacing between the rings is 1.4 mm. The antennas have been analyzed by using electromagnetic software. The matching stubs and metallic strips locations and dimensions have been optimized to get the best VSWR results. The S11 parameter of the metamaterial antenna with metallic strips is presented in **Figure 5**. The antenna bandwidth is around 75% for VSWR better than 2.3:1.

The antenna radiation pattern is shown in **Figure 6**. The 3D computed radiation pattern is shown in **Figure 7**. Directivity and gain of the antenna with SRR are around 5dBi.

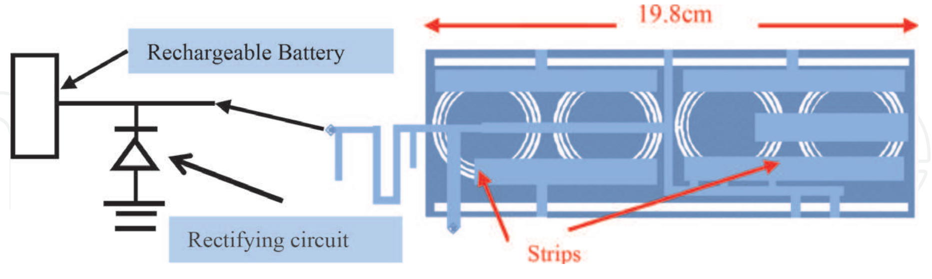

Figure 4.
Wideband antenna with SRR and metallic strips.

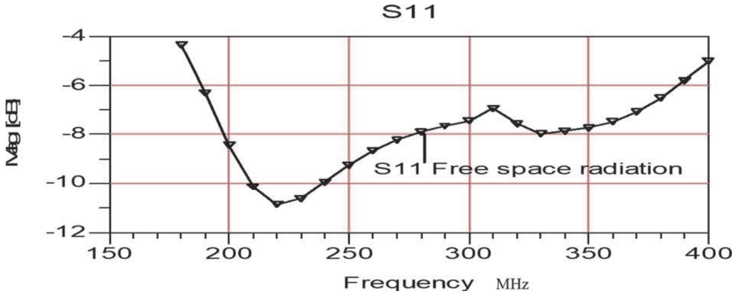

Figure 5.
S11 for antenna with SRR and metallic strips.

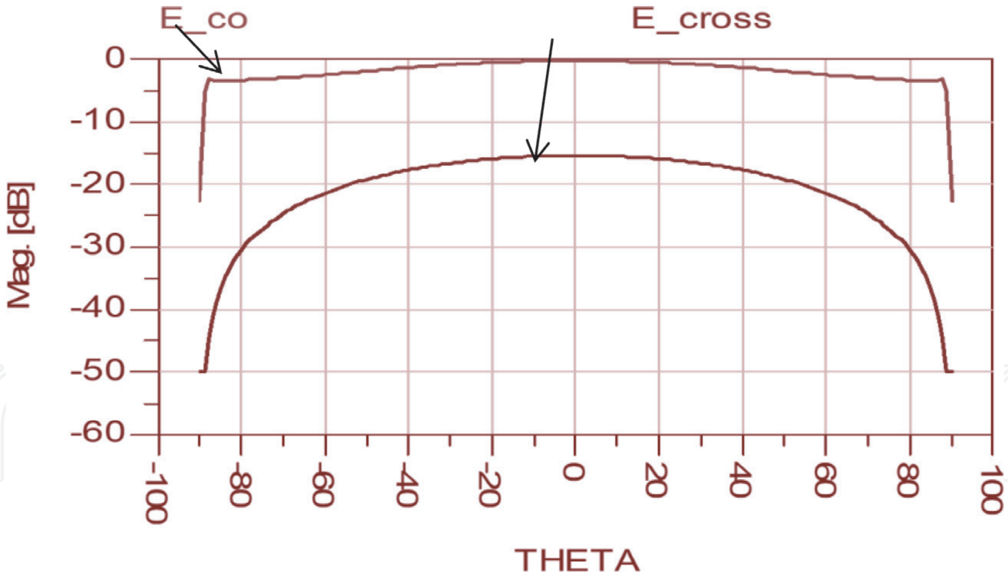

Figure 6.
Radiation pattern for antenna with SRR and metallic strips.

Figure 7.
3D radiation pattern for antenna with SRR.

4. Wideband 400 MHz to 6.4GHz, energy harvesting slot antenna

RF energy in the frequency range from 400 MHz to 6.4GHz may be harvested by a wideband compact T shape slot antenna as presented in **Figure 8**. The slot

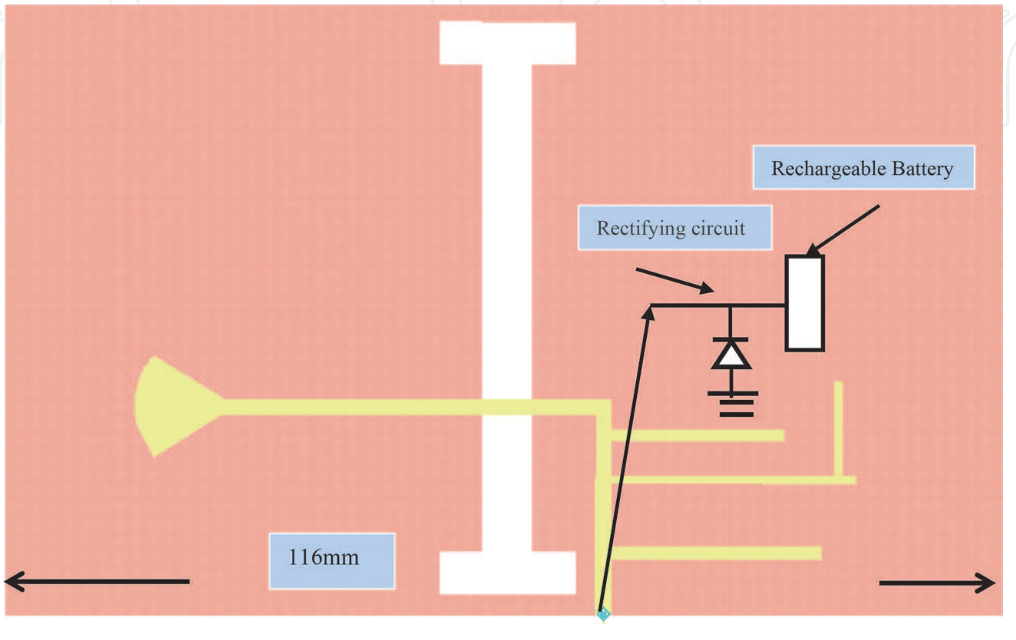

Figure 8.
A ultra-wide band T shape printed harvesting slot antenna.

antenna is printed on a dielectric substrate with dielectric constant of 2.2 and 1.2 mm thick. The dimensions of the slot antenna shown in **Figure 8** are 116x70x1.2 mm. The antenna electrical parameters were calculated and optimized

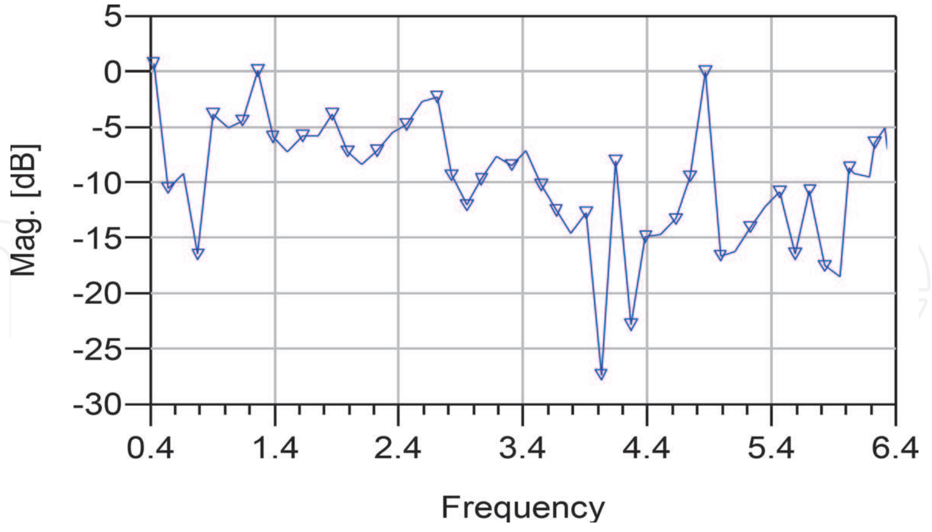

Figure 9.
S11 of a wide band printed T shape energy harvesting slot antenna.

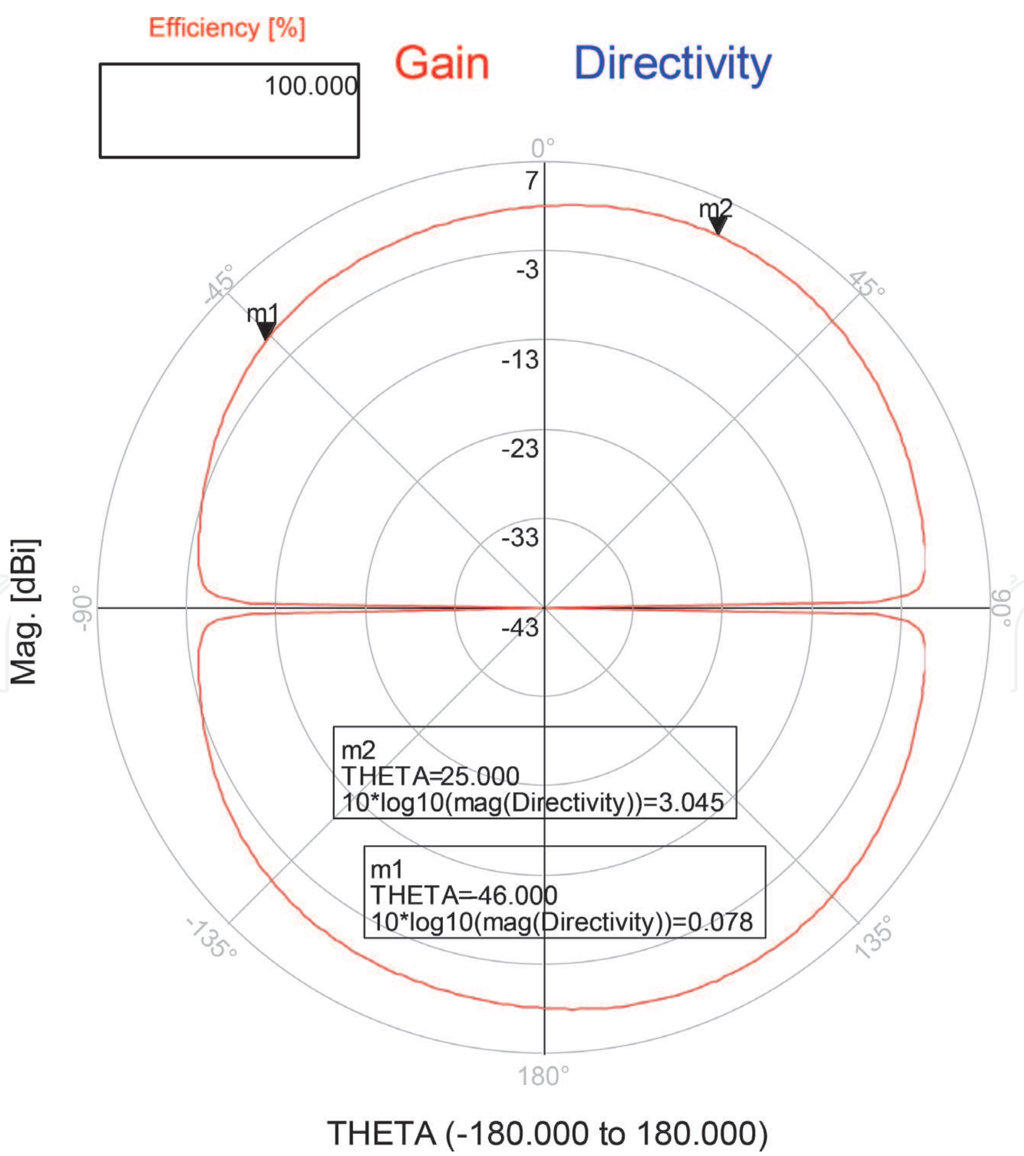

Figure 10.
Radiation pattern of a wide band wearable printed T shape slot antenna at 1.5GHz.

by using ADS software [37]. The S11 parameter of the wideband T shape slot antenna is presented in **Figure 9**. The radiation pattern of the wideband T shape slot antenna at 1.5GHz is shown in **Figure 10**. The antenna gain is 3 dB.

5. New compact ultra-wideband harvesting notch antenna 5.8GHz to 18GHz

A wideband notch antenna with fractal structure was developed. The notch antenna is printed on a dielectric substrate with dielectric constant of 2.2 and 1.2 mm thick. The notch antenna is presented in **Figure 11**. The antenna volume is 11x7.7x1.2 mm. The antenna resonates from 5.8GHz to 18GHz. The antenna bandwidth is around 200% for VSWR better than 3.5:1, as presented in **Figure 12**. The notch antenna VSWR is better than 3:1 for more than 90% of the frequency range

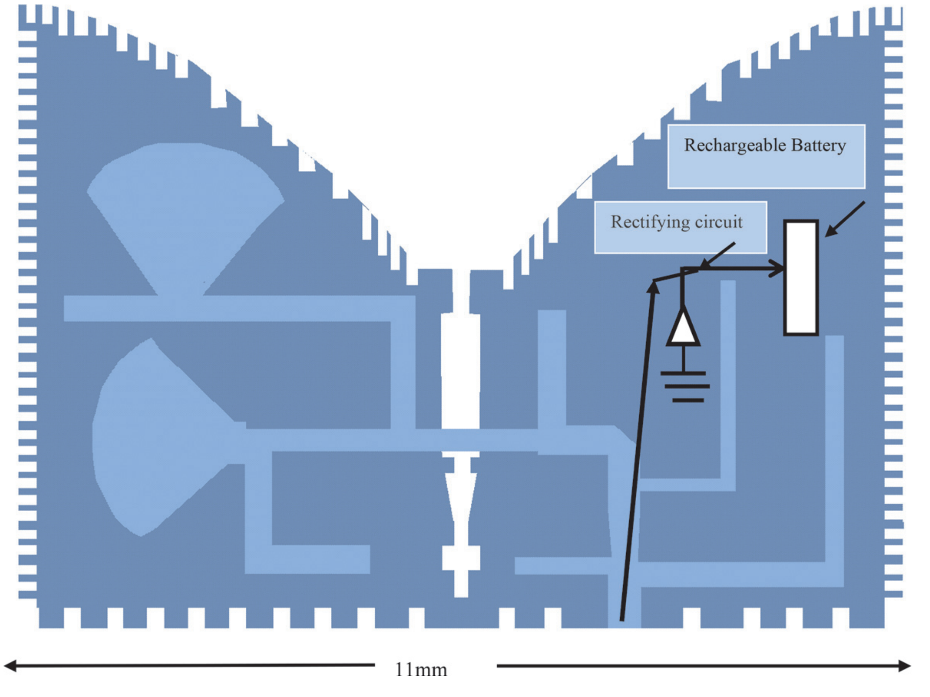

Figure 11.
A wideband 5.8GHz to 18GHz notch antenna with fractal structure.

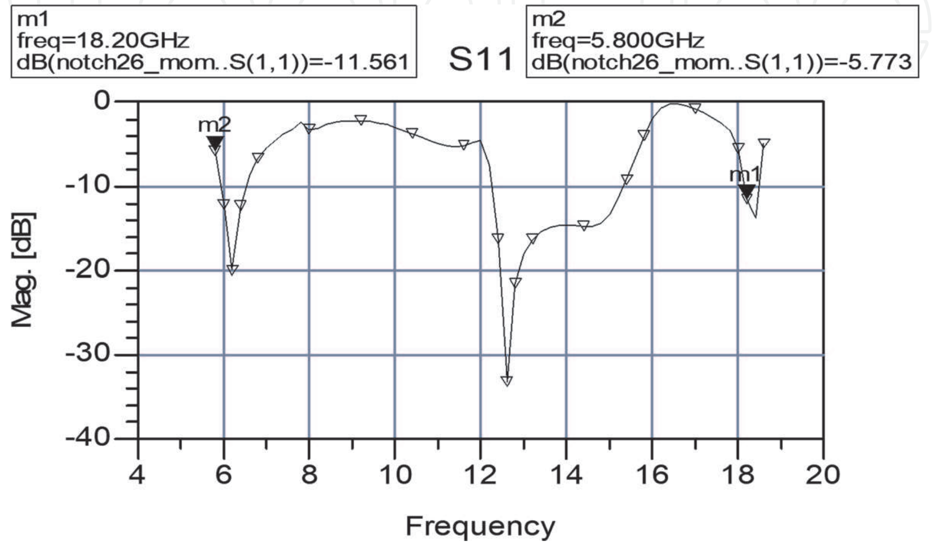

Figure 12.
A wideband 5.8GHz to 18GHz notch antenna with fractal structure, S11 results.

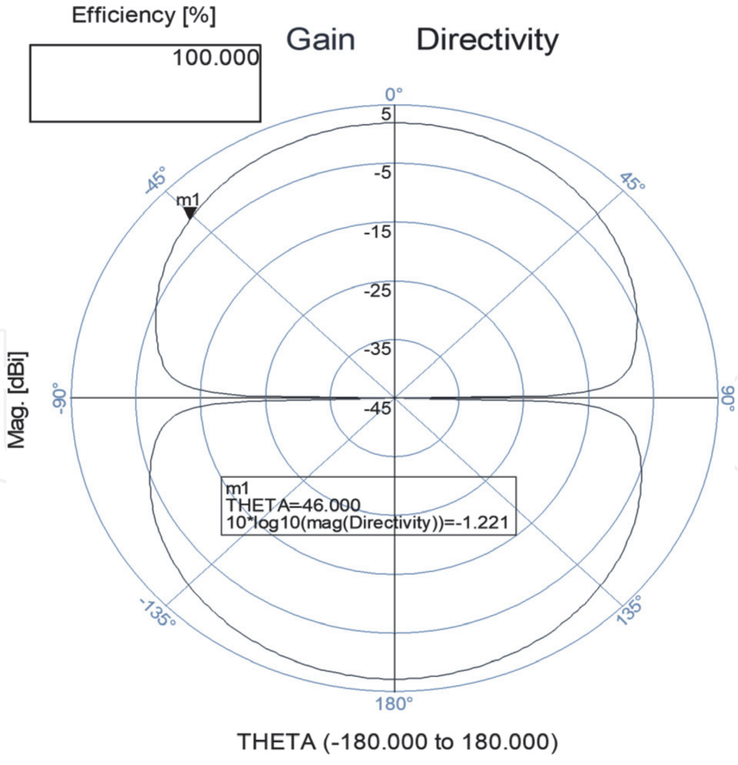

Figure 13.
Radiation pattern of the wideband notch antenna with fractal structure at 8GHz.

from 5.8GHz to 18GHz. The radiation pattern of the wideband notch antenna with fractal structure at 8GHz is shown in **Figure 13**. The antenna beam width at 6GHz is around 84°. The antenna gain, at 6GHz 3.5dBi. The antenna matching network was tuned and optimized to get better S11 results at 16GHz to 18GHz. The length and width of the stubs were tuned and optimized to get better S11 results at 16GHz to 18GHz.

6. Wideband energy harvesting systems and applications

As shown in **Figure 1** the programable array energy harvesting system consists of wideband programable antenna network, a rectifying circuit, and a rechargeable battery. A rectifier converts AC energy, alternating current AC, to DC energy (direct current DC). The popular rectifiers are half wave rectifier or full wave rectifier, [1–4]. A Half wave rectifier is presented in **Figure 14**. A half-wave rectifier conducts only during the positive voltage half cycle. It allows only one half of the electromagnetic waveform to pass through the load. The rectifier output DC voltage, V_{ODC}, is given in Eq. (6). The rectifier output voltage may be improved by connecting a capacitor in shunt to the resistor. The half wave rectifier with a capacitor is shown in **Figure 14**. *Vripple* is given in Eq. (7).

$$\begin{aligned} V_{O,DC} &= \frac{1}{2\pi}\int_0^{2\pi} V_O^{MAX}\sin(\omega t)d(\omega t); \quad \omega = 2\pi f \\ V_O &= V_S - V_{DON} \approx V_S; \quad {V_O}^{MAX} = V_m \\ V_{ODC} &= V_m/\pi \end{aligned} \tag{6}$$

$$Vripple = Vr = Vmax - Vmin = \frac{VDC}{fCR} \tag{7}$$

The time constant τ should be lower than T. Where, $\tau = RC \ll T$. The half wave rectifier efficiency is 40.6%. Only 40.6% of the input AC power is converted into DC power. Where rf is the diode resistance is negligible as compared to R.

A Half wave bridge rectifier is shown in **Figure 15**. The bridge full wave rectifier circuit is used to convert AC energy to DC energy and for DC power suppliers. The bridge rectifier consists of four diodes D1 through D4, as shown in **Figure 15**. During the positive input half cycle, terminal A will be positive and terminal B will be negative. Diodes D1 and D2 will become forward biased and D3 and D4 will be reversed biased. The rectifier output DC voltage, $V_{ODC} = 2V_m/\pi$, The rectifier output voltage may be improved by connecting a capacitor in shunt to the resistor as shown in **Figure 15**.

The half wave rectifier efficiency is 81.2% as presented in Eq. (8). This means that only 81.2% of the input AC power is converted into DC power. The harvested voltage from the three antennas is V_{Total} as written in Eq. (9). The total DC energy is P_{Total} as written in Eq. (10). The actual harvested energy is P as written in Eq. (11).

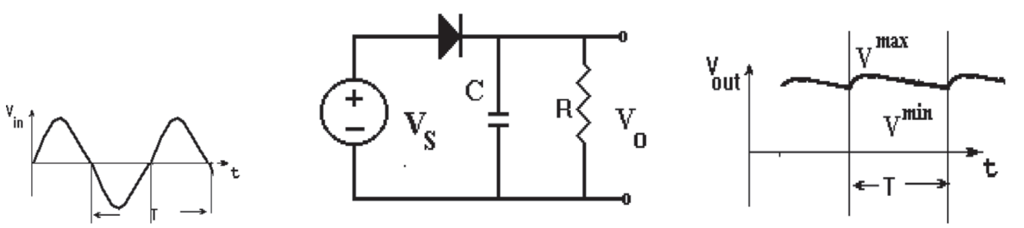

Figure 14.
Half wave voltage rectifier with a capacitor.

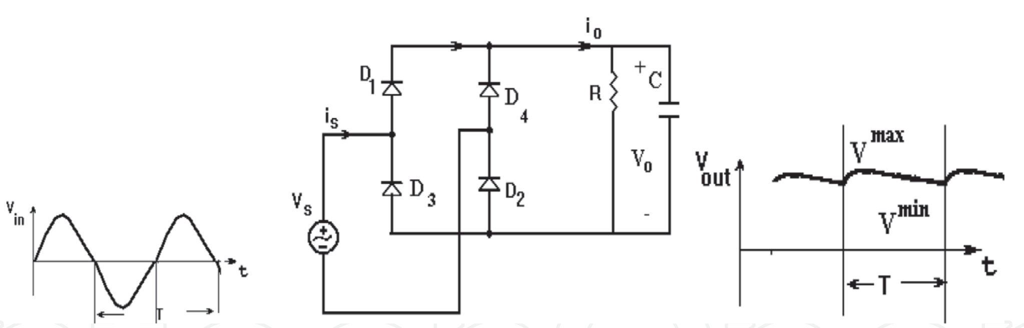

Figure 15.
Full wave bridge voltage rectifier with a capacitor.

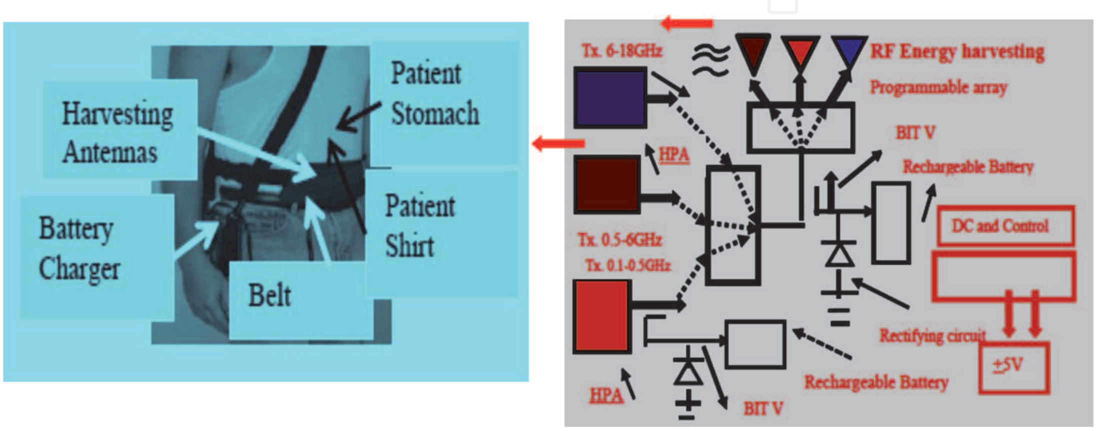

Figure 16.
Ultra-wideband RF system with energy harvesting modules for 5G and medical applications.

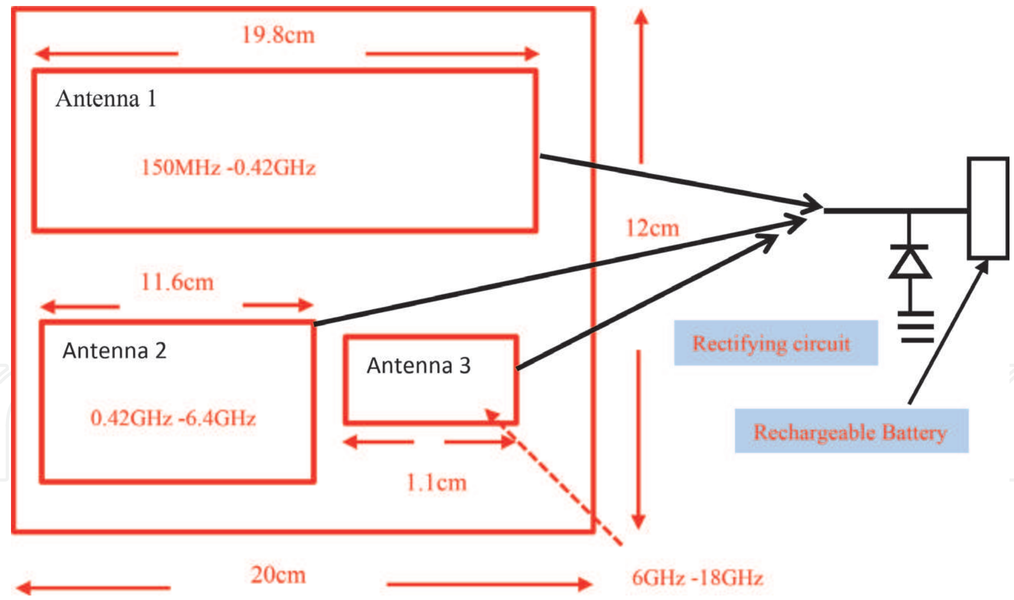

Figure 17.
Wideband RF energy harvesting panel.

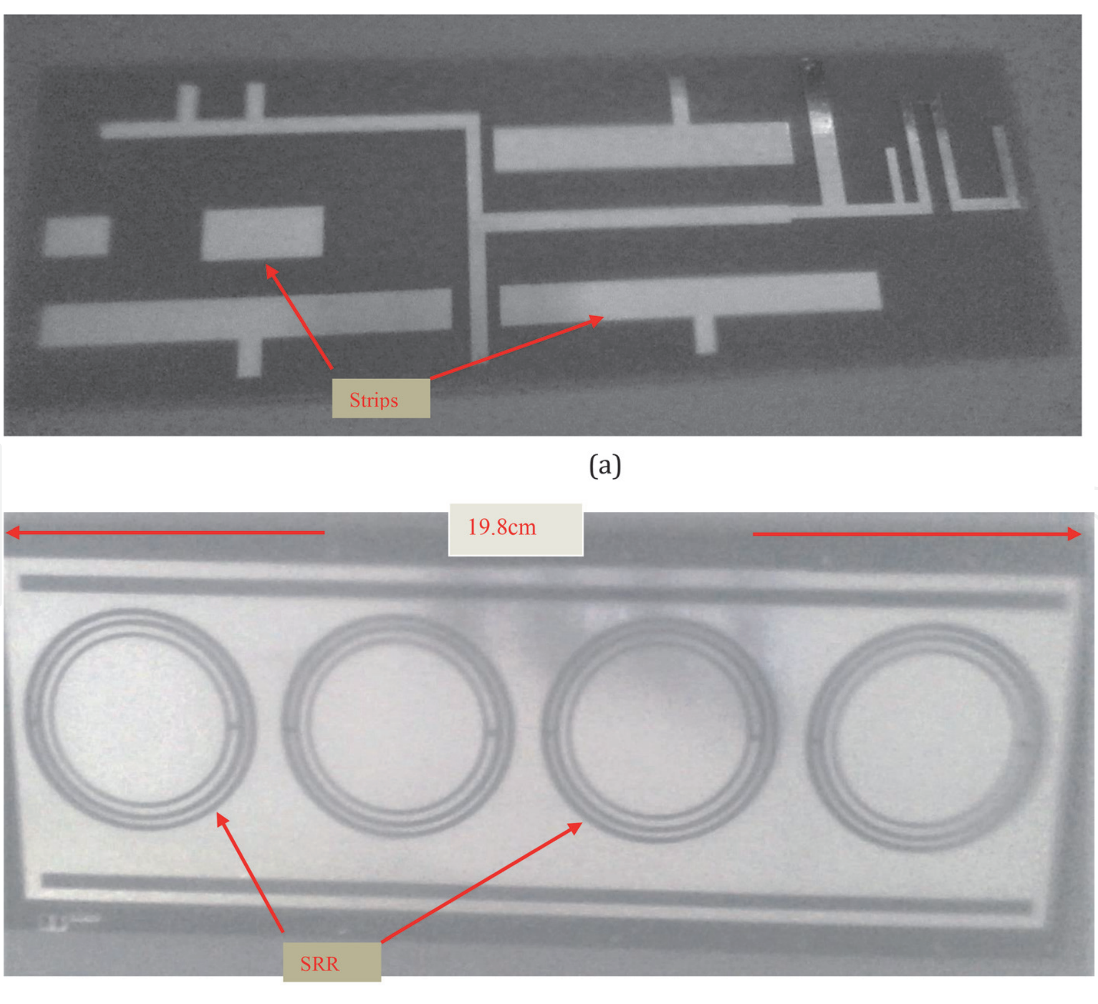

Figure 18.
Wideband energy harvesting metamaterial UHF antenna. (a) the antenna feed network and metallic strips. (b) Dual polarized UHF energy harvesting metamaterial antenna with four SRRs.

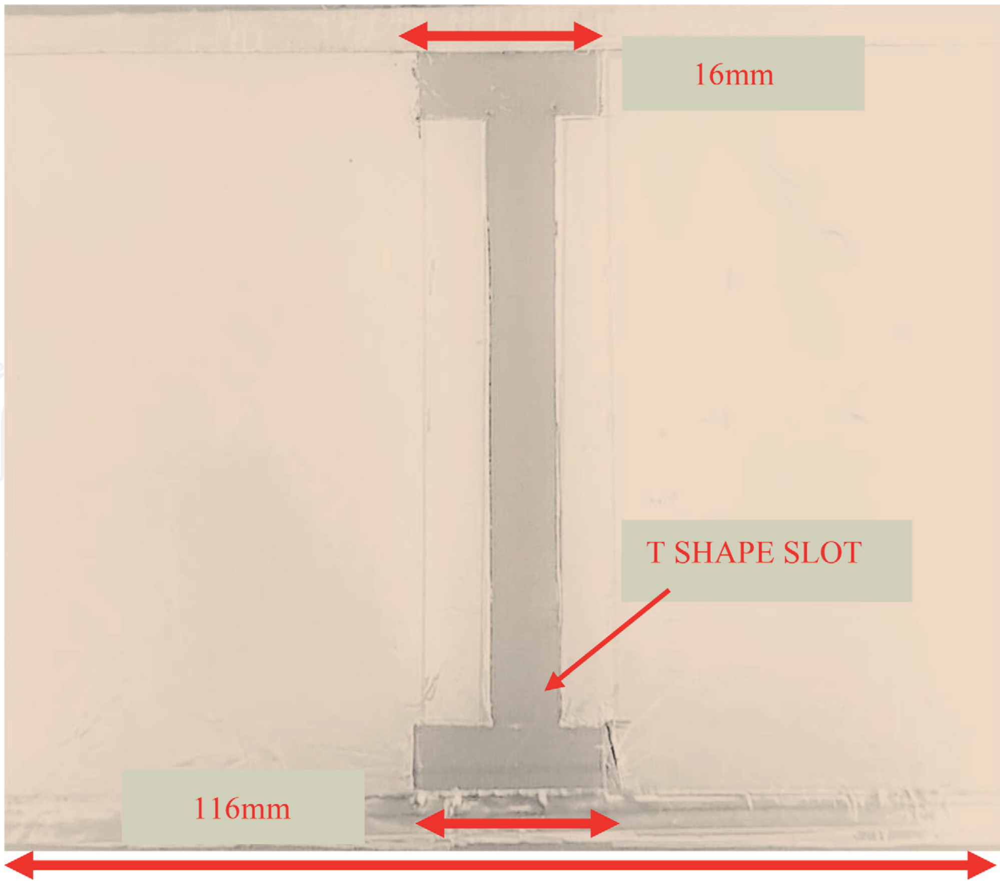

Figure 19.
A photo of wideband energy harvesting slot antenna, 400 MHz - 6 GHz.

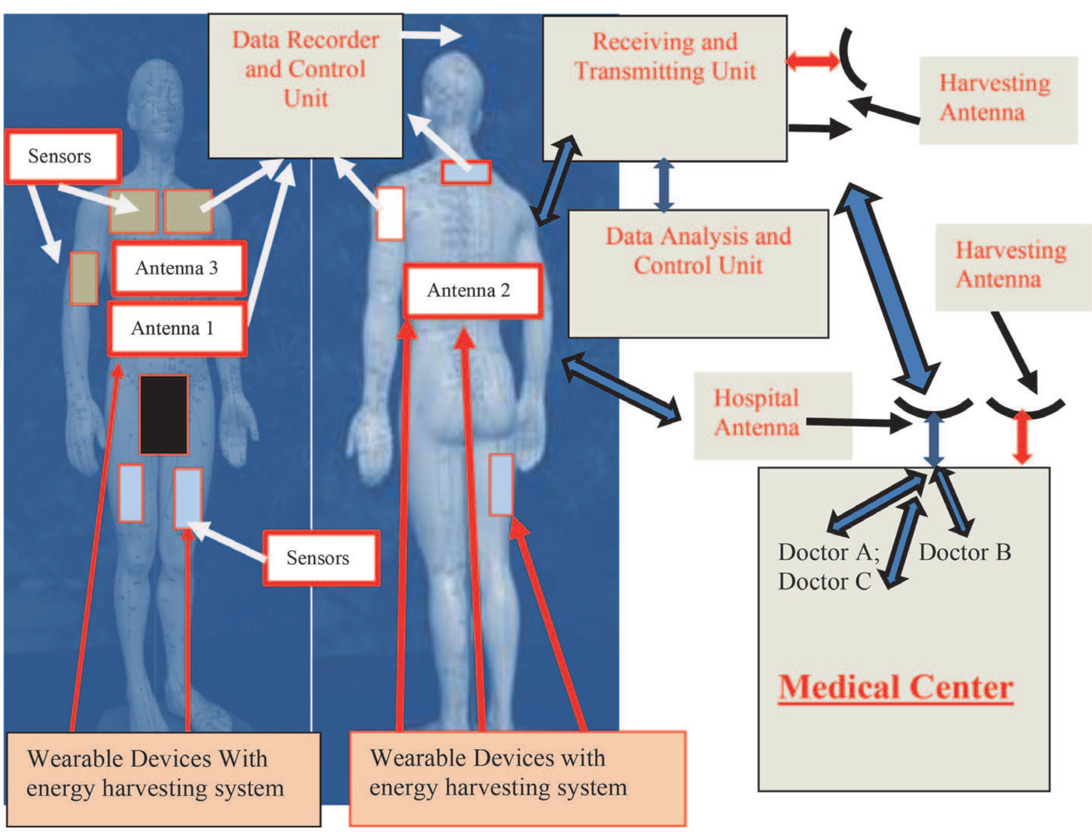

Figure 20.
Wearable body area network with energy harvesting system for medical applications.

$$\eta = \frac{\text{DCoutputpower}}{\text{ACinputpower}} = \frac{\left(\frac{2I_m}{\pi}\right)^2 R}{\left(\frac{I_m}{2}\right)^2 (R + rf)}\ 0.812 \tag{8}$$

$$V_{Total} = V_1 + V_2 + V_3 \tag{9}$$

$$P_{Total} = \frac{V_{Total}^2}{R} = I_m^2 R \tag{10}$$

$$P = 0.81 P_{Total} = 0.81 \frac{V_{Total}^2}{R} = 0.81 I_m^2 R \tag{11}$$

A Schottky diode may be used in the rectifier circuit. Schottky diodes are semiconductor diodes which has a low forward voltage drop and a very fast switching action. There is a small voltage drop across the diode terminals when current flows through the diode. The voltage drop of a Schottky diode is usually between 0.15 and 0.4 volts. This lower voltage drop provides better system efficiency and higher switching speed. A normal diode has a voltage drop between 0.6 to 1.7 volts. RF energy harvesting systems can be used to charge wearable devices. Ultra-Wideband RF System with energy harvesting modules for 5G and Medical applications is shown in **Figure 16**. **Figure 16** presents a wearable harvesting system with a wearable battery charger attached to a patient shirt. A wideband energy Harvesting panel with three antennas is presented in **Figure 17**. The panel dimensions are 20x12x0.02 cm. This panel can harvest energy in frequencies from 150 MHz to 18GHz as part of communication, medical, and IOT systems.

Figure 18 presents a photo of a wideband metamaterial antenna with metallic strips, 150 MHz −0.5GHz. **Figure 18a** presents the antenna feed network and the metallic strips. **Figure 18b** presents the dual polarized metamaterial antenna with four SRRs. **Figure 19** presents a photo of a wideband T shape slot antenna, 420 MHz −6.4GHz. These antennas can be used to harvest RF energy to charge wearable devices and sensors. The UHF dual polarized antenna can be attached to the patient stomach or back. The wideband T shape slot can be attached to the patient stomach or back. The wideband compact notch antenna can be also attached to the patient stomach or back. These antennas provide a wideband wearable communication system with a wideband RF harvesting system. Wearable Body Area Network with energy harvesting system for medical applications is presented in **Figure 20**.

A comparison of computed and measured results of compact wearable antennas for medical, 5G and IoT systems is listed in **Table 4**. Printed dipoles with and without SRR were presented in [9–10].

Antenna	Frequency (GHz)	Bandwidth %	VSWR	Computed Gain dBi	Measured Gain dBi
Printed dipole [9]	0.43	5–10	2:1	2–3	2–3
Dipole with SRR	0.4	8–12	2:1	5–7	5–7
Dipole (SRR and strips) [10]	0.14 to 0.42	UWB	2.5:1	5–7.5	5–7.5
Slot [10]	1 to 4	UWB	2:1	3	3
T shape slot [10]	0.4 to 6.4	UWB	3:1	3	3
Notch [10]	6 to 18	UWB	3:1	3	2–3

Table 4.
Comparison of electrical characteristics of energy harvesting antennas [9–10].

7. Conclusions

This chapter presents new Ultra-Wideband energy harvesting system and antennas in frequencies ranging from 0.15GHz to 18GHz. Three wideband antennas cover the frequency range from 0.15GHz to 18GHz. A wideband metamaterial antenna with metallic strips covers the frequency range from 0.15GHz to 0.42GHz. A wideband slot antenna covers the frequency range from 0.4GHz to 6.4GHz. A wideband fractal notch antenna covers the frequency range from 6GHz to 18GHz. The electromagnetic energy is converted to DC energy that may be employed to charge batteries, wearable medical devices, IOT, laptop batteries and commercial Body Area Networks, BANs. The harvesting energy system operates as a dual mode RF harvesting system. The harvesting unit can be part of a medical, IOT, computer, and smartphone. The notch and slot antennas were analyzed by using 3D full-wave software. Harvested power from RF transmitting links is usually lower than 0.1 $\mu W/cm^2$. All antennas presented in this chapter can operate also as active antennas. Active antennas may improve the energy harvesting system efficiency. The wideband RF energy harvesting system consists of wideband antenna, DC and control unit, a rectifying circuit, and a rechargeable battery. The harvesting energy system operates as a Dual Mode Energy harvesting system. The active devices DC bias voltages are supplied by the communication system. The wideband programmable energy harvesting panel can harvest energy in frequencies from 150 MHz to 18GHz as part of communication, medical, and IOT systems. The antennas presented in this chapter provide a wideband wearable communication system with a wideband RF harvesting system. There is a good agreement between computed and measured results.

Author details

Albert Sabban[1,2]

1 Kinneret Academic College, Galilee, Israel

2 Ort Braude College, Karmiel, Israel

*Address all correspondence to: sabban@netvision.net.il

References

[1] J. A. Paradiso and T. Starner, "Energy scavenging for mobile and wireless electronics," IEEE Pervasive Computing, vol. 4, no. 1, pp. 18–27, 2005.

[2] C. R. Valenta and G. D. Durgin, "Harvesting wireless power: survey of energy-harvester conversion efficiency in far-field, wireless power transfer systems," IEEE Microwave Magazine, vol. 15, no. 4, pp. 108–120, 2014.

[3] P. Nintanavongsa, U. Muncuk, D. R. Lewis, and K. R. Chowdhury, "Design optimization and implementation for RF energy harvesting circuits," IEEE Journal on Emerging and Selected Topics in Circuits and Systems, vol. 2, no. 1, pp. 24–33, 2012.

[4] K. K. A. Devi, S. Sadasivam, N. M. Din, and C. K. Chakrabarthy, "Design of a 377 Ω patch antenna for ambient RF energy harvesting at downlink frequency of GSM 900," in Proceedings of the 17th Asia Pacific Conference on Communications (APCC '11), pp. 492–495, Sabah, Malaysia, October 2011.

[5] R. A. Rahim, F. Malek, S. F. W. Anwar, S. L. S. Hassan, M. N. Junita, and H. F. Hassan, "A harmonic suppression circularly polarized patch antenna for an RF ambient energy harvesting system," in Proceedings of the IEEE Conference on Clean Energy and Technology (CEAT '13), pp. 33–37, IEEE, Lankgkawi, Malaysia, November 2013.

[6] M. Krakauskas, A. M. A. Sabaawi, and C. C. Tsimenidis, "Suspended patch microstrip antenna with cut rectangular slots for RF energy harvesting," in Proceedings of the 10th Loughborough Antennas and Propagation Conference (LAPC '14), pp. 304–307, Loughborough, UK, November 2014.

[7] Albert Sabban, "Low visibility Antennas for communication systems" , TAYLOR & FRANCIS group, 2015, USA.

[8] Albert Sabban (2018). "Wearable Communication Systems and Antennas for Commercial, Sport, and Medical Applications". IET Publication, December 2018.

[9] Albert Sabban, "Wideband RF Technologies and Antenna in Microwave Frequencies", Wiley Sons, July 2016, USA.

[10] Albert Sabban. *Novel Wearable Antennas for Communication and Medical Systems*; Taylor & Francis Group: Boca Raton, FL, USA, 2017.

[11] A. Sabban and K.C. Gupta, "Characterization of Radiation Loss from Microstrip Discontinuities Using a Multiport Network Modeling Approach", I.E.E.E Trans. on M.T.T, Vol. 39,No. 4,April 1991, pp. 705–712.

[12] A. Sabban,"A New Wideband Stacked Microstrip Antenna", I.E.E.E Antenna and Propagation Symp., Houston, Texas, U.S.A, June 1983.

[13] A. Sabban, E. Navon "A MM-Waves Microstrip Antenna Array", I.E.E.E Symposium, Tel-Aviv, March 1983.

[14] Balanis, C.A. "Antenna Theory: Analysis and Design", 2nd Edition. Wiley, 1996

[15] A. Sabban, PhD Thesis, Multiport Network Model for Evaluating Radiation Loss and Coupling Among Discontinuities in Microstrip Circuits, University of Colorado at Boulder, January 1991.

[16] Inventors: Albert Sabban, *Microstrip antenna arrays*, U.S. Patent US 1986/4,623,893, 1986.

[17] A. Sabban, "Wideband Microstrip Antenna Arrays", I.E.E.E Antenna and

Propagation Symposium MELCOM, Tel-Aviv June 1981.

[18] K. Fujimoto, J.R. James, Editors, Mobile Antenna Systems Handbook, Artech House, Boston USA, 1994.

[19] A. Sabban, "New Wideband Notch Antennas for Communication Systems", Wireless Engineering and Technology Journal, pp. 75–82, April 2016.

[20] Inventors: Albert Sabban, Dual polarized dipole wearable antenna, U.S Patent number: 8203497, June 19, 2012, USA.

[21] A. Sabban (2012) Wideband Tunable Printed Antennas for Medical Applications. I.E.E.E Antenna and Propagation Symp., Chicago IL. ,U.S.A, July 2012.

[22] A. Sabban, "New Wideband printed Antennas For Medical Applications" I.E. E.E Trans. on Antennas and Propagation, January 2013, Vol. 61, No. 1, pp. 84–91.

[23] A. Sabban, "Comprehensive Study of Printed Antennas on Human Body for Medical Applications" International Journal of Advance in Medical Science (AMS), Vol. 1, pp. 1–10, February 2013.

[24] R. Kastner, E. Heyman, A. Sabban, "Spectral Domain Iterative Analysis of Single and Double-Layered Microstrip Antennas Using the Conjugate Gradient Algorithm", I.E.E.E Trans. on Antennas and Propagation, Vol. 36, No. 9, Sept. 1988, pp. 1204–1212.

[25] A. Sabban, "Microstrip Antenna Arrays", Microstrip Antennas, Nasimuddin Nasimuddin (Ed.), ISBN: 978–953–307-247-0, InTech, http://www.intechopen.com/articles/show/title/microstrip-antenna-arrays , pp..361–384, 2011.

[26] Lawrence C. Chirwa*, Paul A. Hammond, Scott Roy, and David R. S. Cumming, "Electromagnetic Radiation from Ingested Sources in the Human Intestine between 150 MHz and 1.2 GHz", IEEE Transaction on Biomedical eng., VOL. 50, NO. 4, April 2003, pp 484–492.

[27] D.Werber, A. Schwentner, E. M. Biebl,"Investigation of RF transmission properties of human tissues", Adv. Radio Sci., 4, 357–360, 2006.

[28] Gupta, B., Sankaralingam S., Dhar, S.,"Development of wearable and implantable antennas in the last decade", Microwave Symposium (MMS), 2010 Mediterranean 2010 , Page(s): 251–267.

[29] Thalmann T., Popovic Z., Notaros B. M, Mosig, J.R.," Investigation and desig n of a multi-band wearable antenna", 3rd European Conference on Antennas a nd Propagation, EuCAP 2009. Pp. 462–465.

[30] Salonen, P., Rahmat-Samii, Y., Kivikoski, M.," Wearable antennas in the vicinity of human body", IEEE Ante nnas and Propagation Society Interna tional Symposium, 2004. Vol.1 pp. 467–470.

[31] Kellomaki T., Heikkinen J., Kivikoski, M., " Wearable antennas for FM reception", First European Conference on Antennas and Propaga tion, EuCAP 2006 , pp. 1-6.

[32] A. Sabban, "Comprehensive Study of Printed Antennas on Human Body for Medical Applications" International Journal of Advance in Medical Science (AMS), Vol. 1, pp. 1–10, February 2013.

[33] A. Sabban, "Wideband printed antennas for medical applications" APMC 2009 Conference, Singapore, Dec. 2009.

[34] A. Alomainy, A. Sani et all "Transient Characteristics of Wearable Antennas and Radio Propagation

Channels for Ultrawideband B ody-centric Wireless Communication", I.E.E.E Trans. on Antennas and Propagation, Vol. 57, No. 4, April 2009, pp. 875–884.

[35] M. Klemm and G. Troester, "Textile UWB antenna for Wireless Body Area Networks", I.E.E.E Trans. on Antennas and Propagation, Vol. 54, No. 11, Nov. 2006, pp. 3192–3197.

[36] P. M. Izdebski, H. Rajagoplan and Y. Rahmat-Sami, "Conformal Ingestible Capsule Antenna: A Novel Chandelier Meandered Design", I.E.E.E Trans. on Antennas and Propagation, Vol. 57, No. 4, April 2009, pp. 900–909.

[37] ADS software, Agilent, http://www.home.agilent.com/agilent/product.jspx?cc=IL&lc=eng&ckey=1297113&nid=34346.0.00&id=1297113